

Supplementary Figures

Figure S1. Reduced expression of BMAL1 and CLOCK in ageing IVDs. IHC of BMAL1 and CLOCK on sections of IVDs from 3 and 12 months old mice; n=4. Magnification, 5x left and middle panels, 10x right panels. BMAL1 staining was visible in the AF, but not the CEP, of 12 month old mice. CLOCK staining was largely absent in both AF and CEP in 12 month old mice.

Figure S2. Effects of LPS, IL-1RA, forskolin and TNF α on IVD oscillations. Representative bioluminescence traces of PER2::Luc mouse IVD explants; n=3. (A) LPS treatment (1 μ g/mL, red trace) disrupted the rhythm, which could be rescued by treatment with dexamethasone (100 nM). (B, C) Disrupted circadian rhythm by IL-1 β treatment (5 ng/mL, red trace) was not rescued by application of forskolin (10 μ M), but by pre-treatment with IL-1RA (1 μ g/mL). Arrows indicate time of treatment. (D) Both IL-1 β (5 ng/mL) and TNF α (40 ng/mL) induced strong NF κ B signalling in lung epithelial cells stably transfected with NF κ B::luc reporter. Representative, n=3.

Figure S3. Effects of IL-1 β on endogenous clock gene expression. qPCR of several clock genes, *Adamts1* and *IL-6* in IVD explants upon IL-1 β treatment (5 ng/mL for 4 hours). *, p<0.05; ***, p<0.001, n=4.

Figure S4. Phase clustering analysis of rhythmic genes in mouse IVDs. Clustering analysis was performed using cluster (A) and Rtsne (B) of R package. These analyses revealed 4 main clusters with different peak times (two at night and two during the day). Example genes for each cluster were highlighted. There was a good concordance between these two methods of analysis.

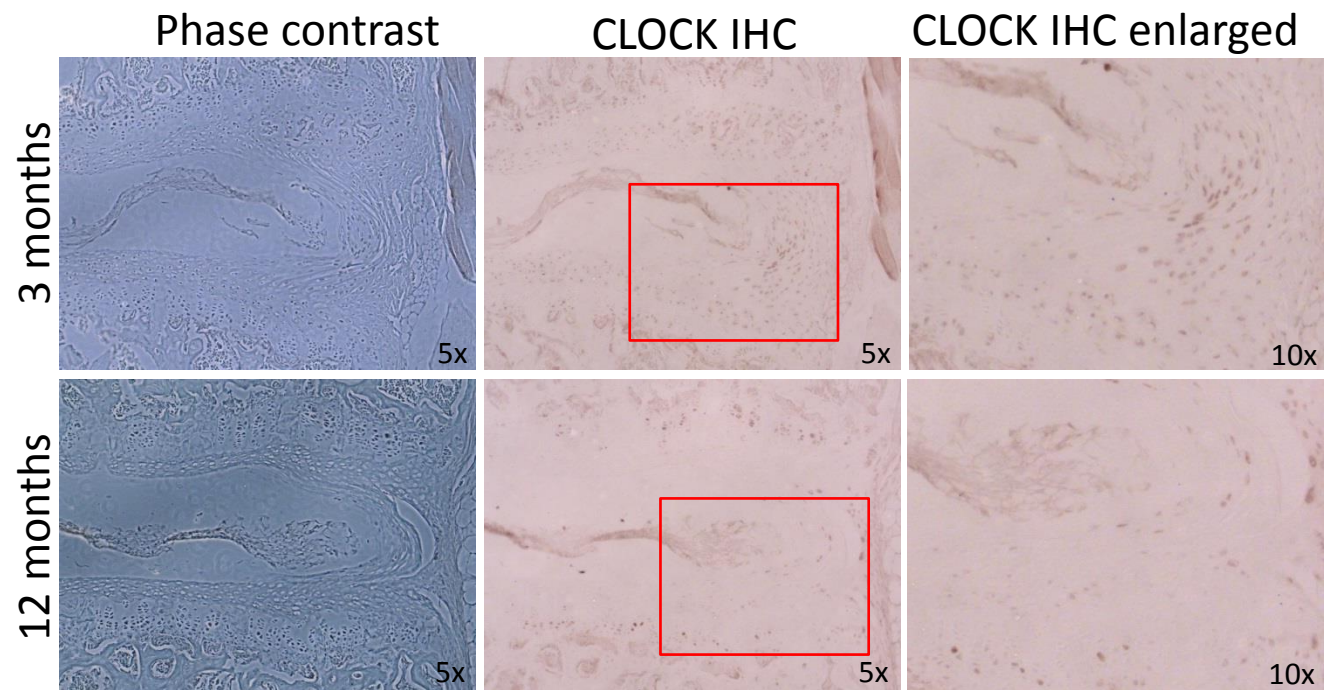
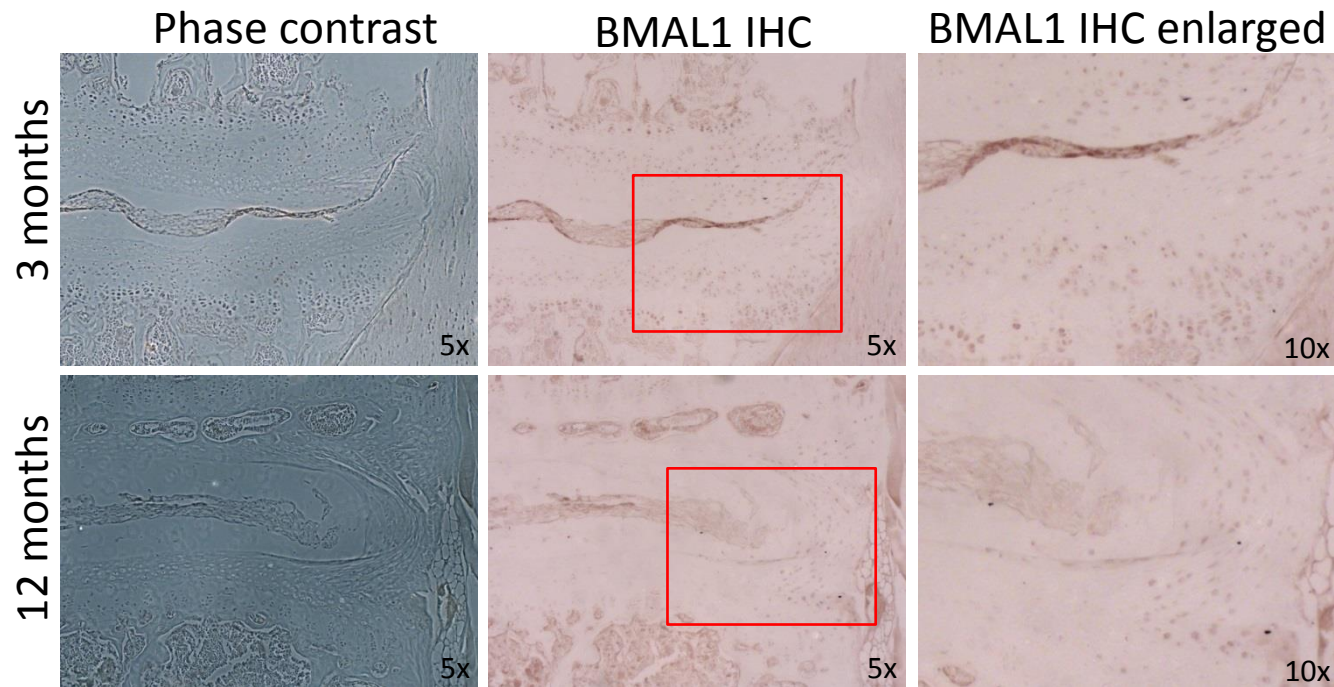
Figure S5. Time course qPCR of β -actin in mouse IVDs. Note the lack of circadian rhythms. Mean and SEM (n = 6).

Figure S6. Early onset of IVD degeneration in IVDs from 6 month old cKO mice. Safranin O/methyl green staining revealed gradual disappearance of CEP in the *Bmal1* cKO mouse (black arrow); n=4.

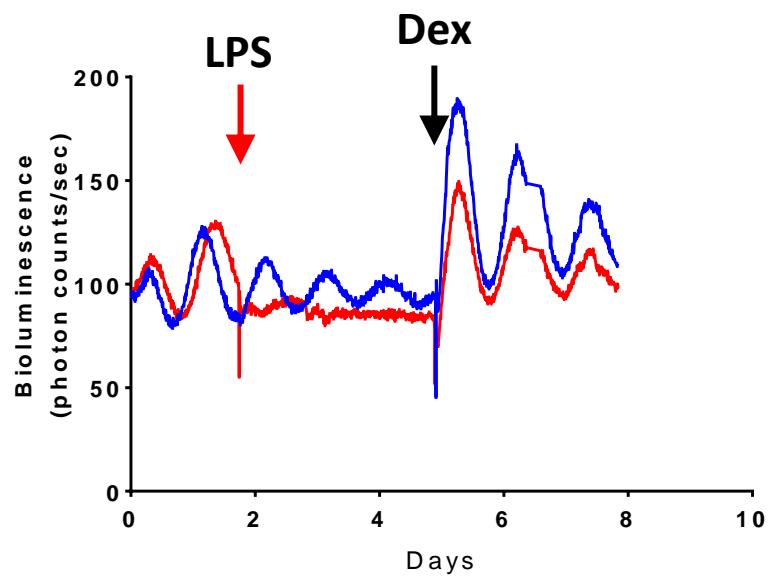
Figure S7. Spontaneous degeneration of IVDs from aged WT mice. Picrosirius red staining and polarised light microscopy were performed on IVDs from 3 and 24 month old wild type mice; n=4. The aged WT mouse IVDs display a phenotype similar to *Bmal1* cKO IVDs, with fibrosis of the outer AF composed of bundles of organised collagen visible under polarised light microscope.

Figure S8. TUNEL staining of IVDs from 12 months old WT and *Bmal1* cKO mice. Note there were no detectable signs of apoptosis in either WT or cKO IVDs. N=4.

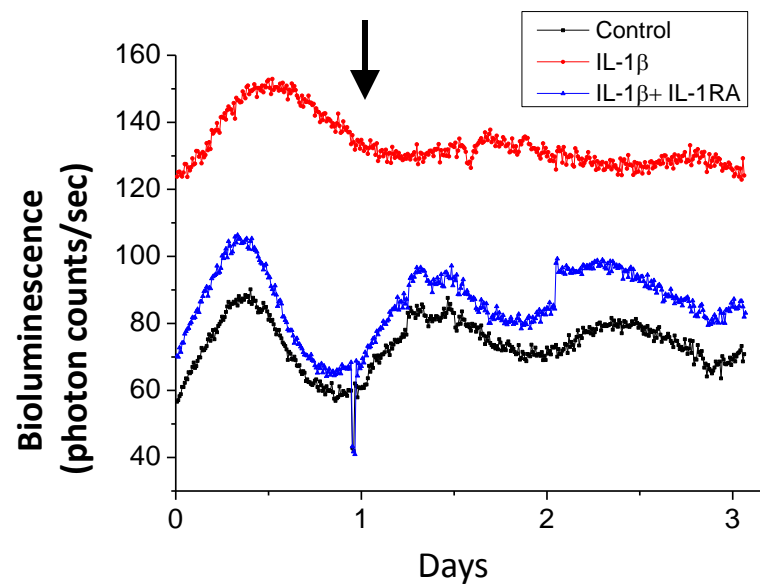
Figure S9. qPCR of catabolic genes in IVDs from 3 months old WT and *Bmal1* cKO mice. Mean and SEM (n = 4). *, p<0.05; **, p<0.01; ***, p<0.001.



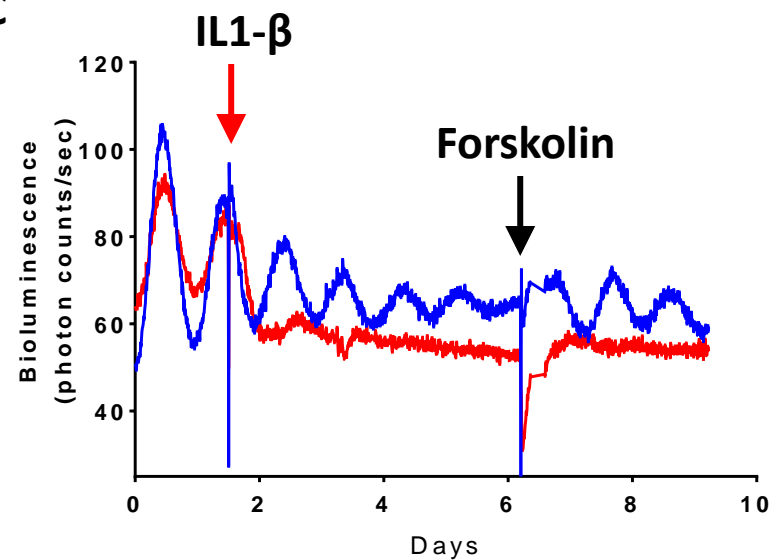
A



B



C



D

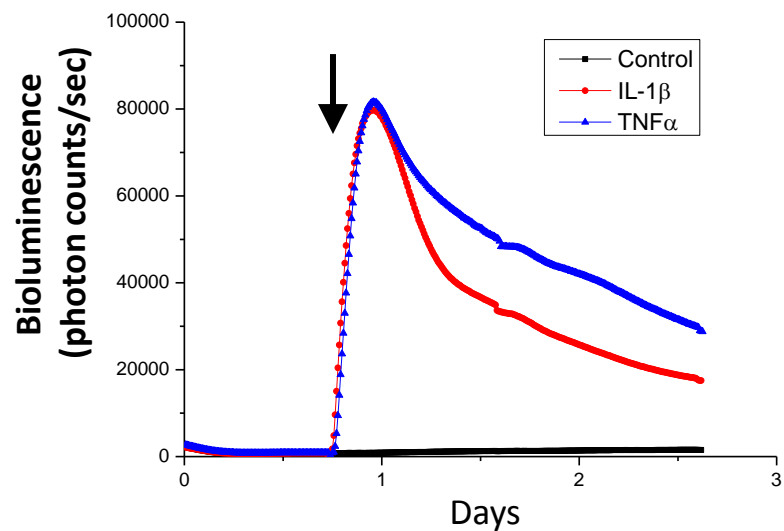


Fig S3

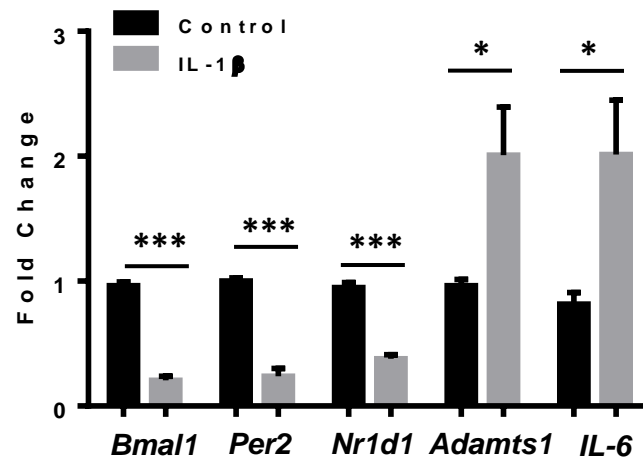


Fig S4

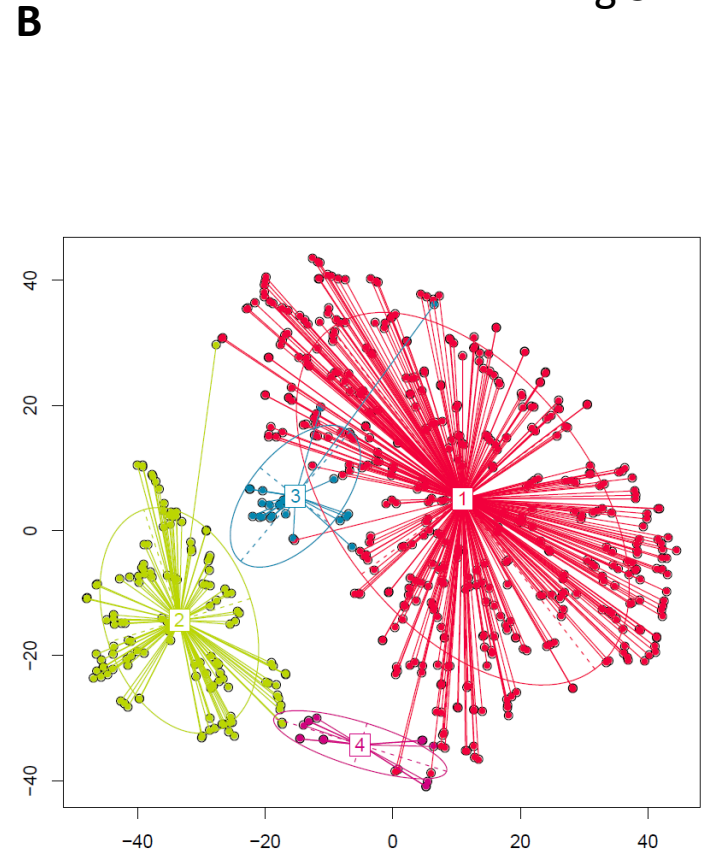
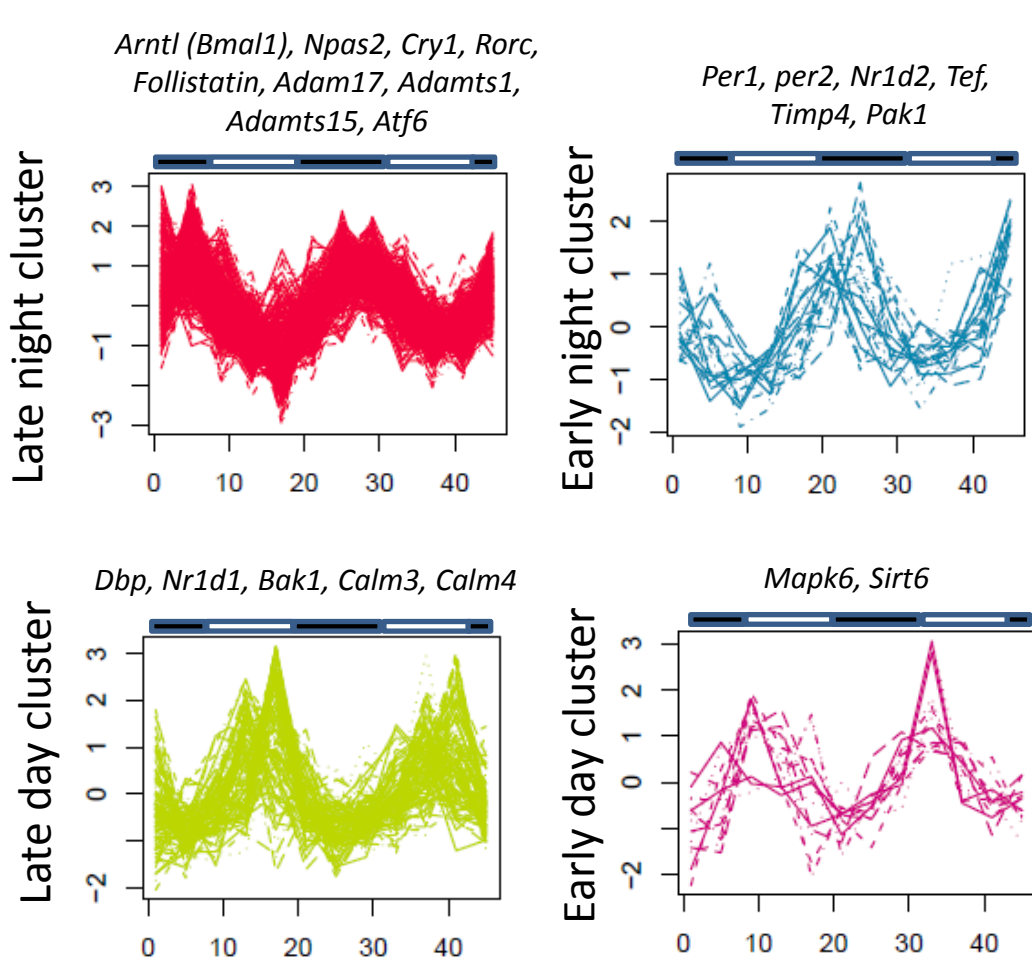


Fig S5

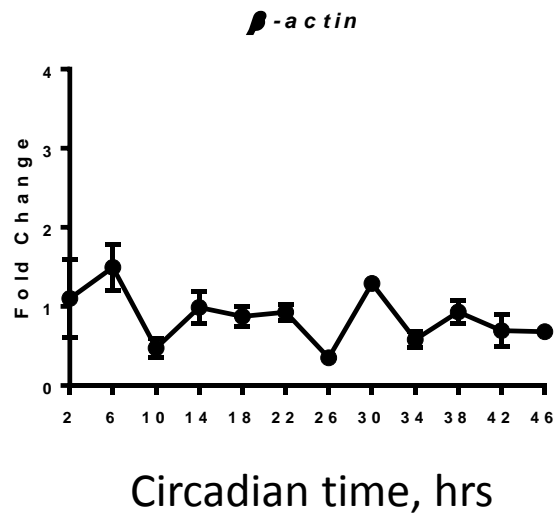


Fig S6

6months

WT

cKO

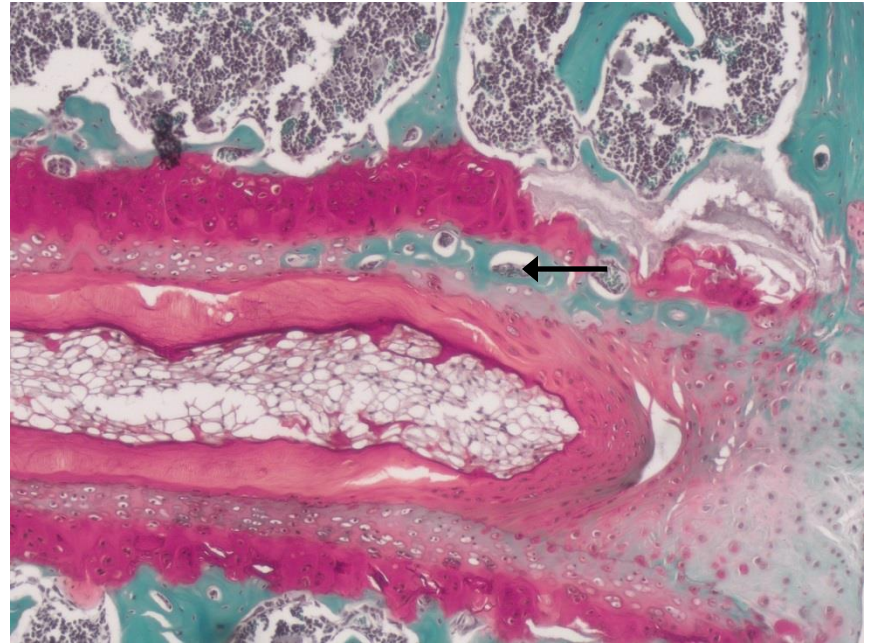


Fig S7

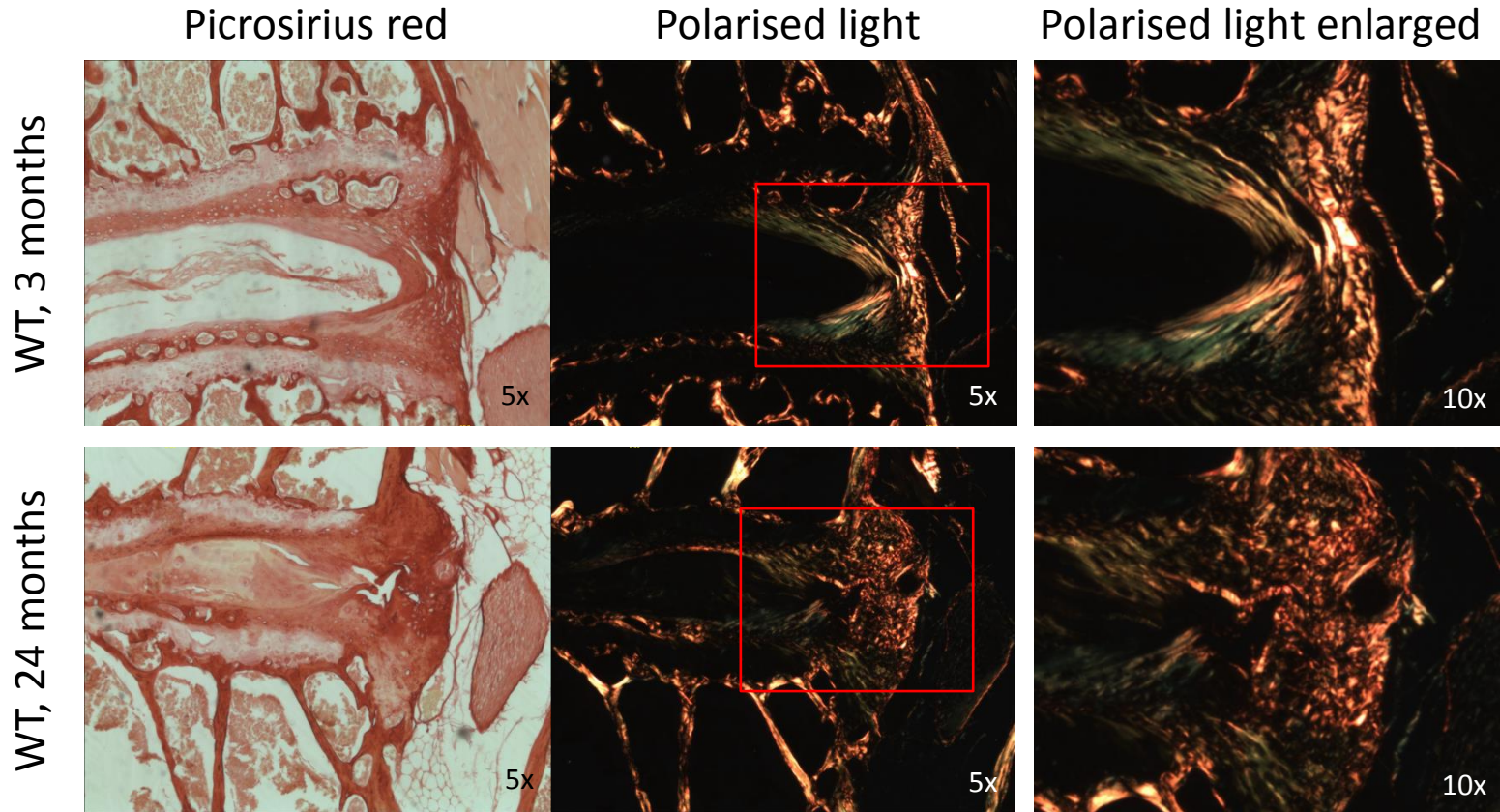


Fig S8

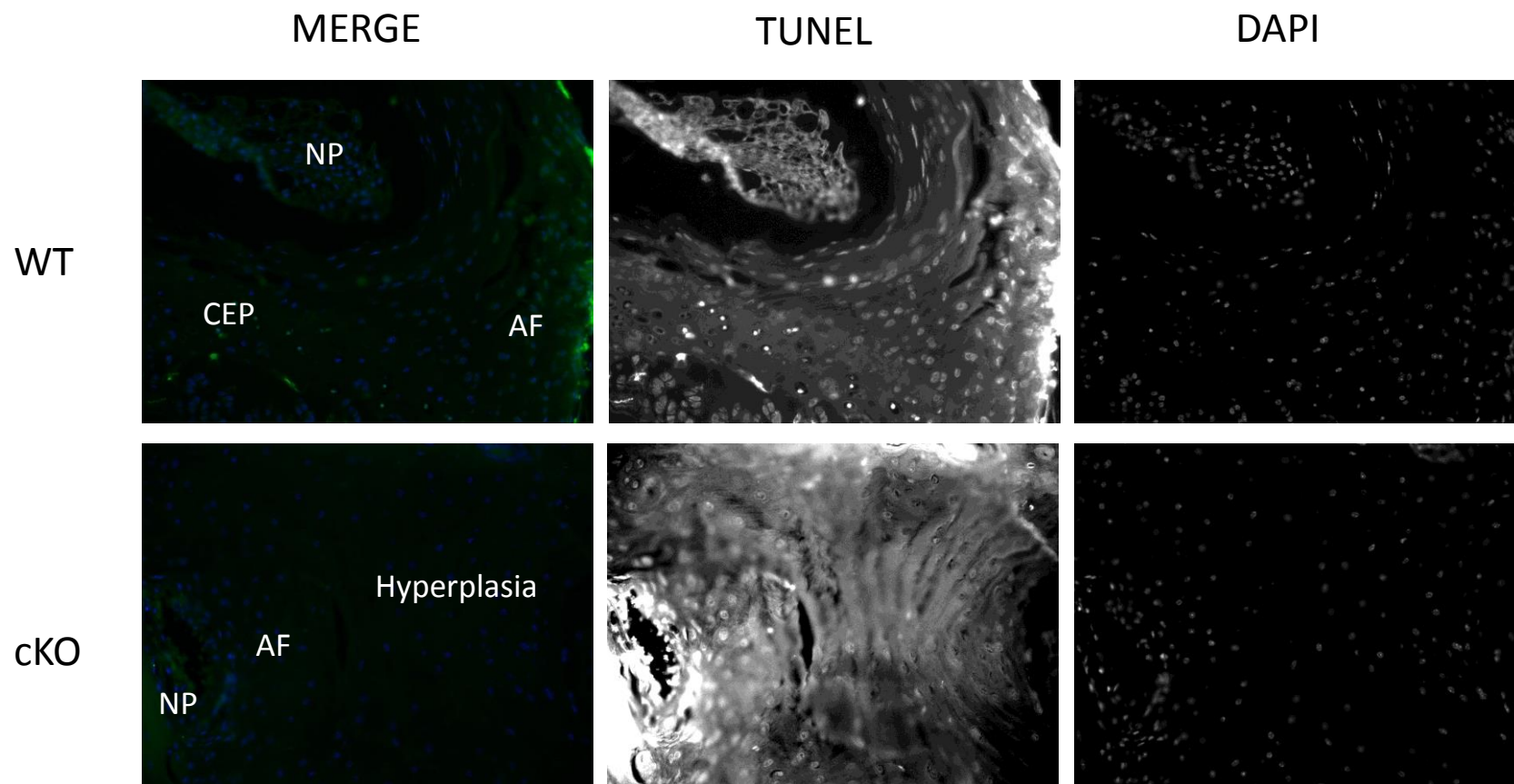


Fig S9

